

Resource-Efficient CSI Prediction: A Gated Fusion and Factorized Projection Approach

Mohammad Hussain, Maedeh Adibag, Dilara Gurer, Gokhan Kalem, Kerim Serin, and Sinem Coleri, *Fellow, IEEE*

Abstract—Accurate Channel State Information (CSI) prediction is essential for dynamic multiple-input multiple-output (MIMO) systems but remains computationally demanding. This letter proposes a resource-efficient predictor that combines a gated recurrent unit (GRU) encoder with Luong attention, a bottleneck gated fusion module, and a Dimension-wise Separable Linear Head (DSLH). The gated fusion module integrates local recurrent features with global attention context, while the DSLH reduces the cost of the output mapping. Evaluated on 3GPP TR 38.901-compliant channels, the proposed model achieves an average NMSE of -13.84 dB with 26% fewer parameters and approximately $2.3\times$ higher inference throughput than a dimension-matched LinFormer baseline. The proposed model is best suited to LOS and mixed-condition scenarios, offering a practical accuracy–efficiency trade-off for short-horizon CSI prediction at moderate sequence lengths.

Index Terms—Channel prediction, gated recurrent unit (GRU), MIMO, resource-efficient deep learning, throughput efficiency.

I. INTRODUCTION

THE performance of MIMO systems relies heavily on accurate CSI. In dynamic wireless environments, the channel varies rapidly, causing CSI to “age” between acquisition and use, leading to severe performance degradation. To mitigate this, deep learning (DL) predictors have been widely adopted to forecast future CSI.

Early DL approaches treated CSI matrices as visual images and employed Convolutional Neural Networks (CNNs) to extract spatial patterns. Vilas Boas *et al.* [1] leveraged this idea for CSI compression, while [2] extended it to 3D-CNNs to capture temporal correlations. Although CNNs model local spatial features effectively, they struggle to capture long-range temporal dependencies, which are important for accurate channel prediction in dynamic environments.

Recurrent neural networks (RNNs) such as long short-term memory (LSTMs) and gated recurrent units (GRUs) better exploit temporal dynamics through hidden-state memory [3], [4], with recent work further improving GRU-based CSI prediction via EVT-based adaptive loss functions [5]. However, standard RNNs process sequences strictly sequentially, which limits parallelization and can amplify error propagation over long horizons.

Transformer-based predictors address RNN limitations including limited parallelization, poor scalability to long se-

quences, and error accumulation through self-attention, enabling parallel processing over the full history. Jiang *et al.* [6] showed that global attention mitigates mobility-related degradation, while physics-inspired variants such as ODEFormer [7] model fading in continuous time. However, transformers incur quadratic attention cost $O(N^2)$, and even efficient variants such as LinFormer [8] retain large embeddings, leading to high parameter and computational overhead that is unsuitable for real-time systems [9].

Prior recurrent and attention-based architectures for CSI prediction already exist, including dual-attention LSTMs for industrial IoT [10], adaptive bidirectional GRUs for underwater MIMO [11], attention-enhanced GRUs for deep-space channels [12], and dynamic graph neural networks for massive MIMO [13]. Rather than proposing GRU–attention itself as a new idea, this paper focuses on a resource-efficient CSI prediction architecture that combines a GRU encoder, Luong-style attention, bottleneck gated fusion, and a DSLH output head, and evaluates this combination under standardized 3GPP conditions. The resulting design targets short-horizon prediction with a favorable balance between accuracy, model size, and inference efficiency. The proposed architecture uses bottleneck gated fusion to adaptively combine encoder states with global attention context before the DSLH head. Compared to fixed linear fusion, the learned gate is more flexible, while DSLH provides a compact alternative to a dense output head. The specific contributions of this letter are as follows:

- *Bottleneck gated fusion*: A lightweight module that combines each time-step feature with a shared attention context using a learned gate. Results show a 0.66 dB improvement over simple linear fusion.
- *DSLH with recurrent encoders*: We show that DSLH works well with recurrent models when attention and gated fusion are used to improve the sequence features. This allows efficient multi-step prediction without needing a large dense output layer.
- *3GPP accuracy–efficiency evaluation*: The proposed model achieves best mean NMSE in LOS and mixed-condition scenarios with 26% fewer parameters and $2.3\times$ higher throughput than LinFormer, evaluated across five 3GPP TR 38.901 scenarios.

The remainder of this letter is organized as follows: Section II details the system model. Section III describes the proposed architecture. Section IV presents the experimental evaluation, including ablation studies, complexity analysis, and accuracy assessments, in various 3GPP scenarios. Section V concludes the paper.

M. Hussain, M. Adibag, and S. Coleri are with the Department of Electrical and Electronics Engineering, Koç University, Istanbul, Turkey (email: {mohussain25, mbag24, scoleri}@ku.edu.tr). D. Gurer and G. Kalem are with Turkcell (email: {dilara.gurer, gokhan.kalem}@turkcell.com.tr). K. Serin is with Opticoms (email: kerim.serin@opticoms.de). This work is supported by the Scientific and Technological Research Council of Turkey (TUBITAK) 1711 Project AI-PG5 #3247019.

II. SYSTEM MODEL

A. MIMO Channel and Notation

We consider a downlink narrowband MIMO channel observed at discrete time index t ,

$$\mathbf{H}_t \in \mathbb{C}^{R \times T}, \quad (1)$$

where T and R denote the number of transmit and receive antennas, respectively. We focus on a single representative subcarrier.

The channel is modeled using a path-resolved representation. Let $\mathbf{H}_{t,p} \in \mathbb{C}^{R \times T}$ denote the contribution of path $p \in \{1, \dots, P\}$ at time t , where P is the total number of multipath components. The effective (path-collapsed) channel is defined as

$$\mathbf{H}_t^{(\text{eff})} \triangleq \sum_{p=1}^P \mathbf{H}_{t,p}. \quad (2)$$

B. Input and Output Representation

At each time t , the effective channel matrix $\mathbf{H}_t^{(\text{eff})}$ is converted to a real-valued representation by vectorizing and stacking its real and imaginary components:

$$\mathbf{h}_t^{(r)} \triangleq \begin{bmatrix} \Re\{\text{vec}(\mathbf{H}_t^{(\text{eff})})\} \\ \Im\{\text{vec}(\mathbf{H}_t^{(\text{eff})})\} \end{bmatrix} \in \mathbb{R}^{2RT}. \quad (3)$$

To incorporate mobility information, the scalar UE speed v_t is appended to form the per-time-step input feature vector:

$$\mathbf{x}_t = [(\mathbf{h}_t^{(r)})^\top, v_t]^\top \in \mathbb{R}^D, \quad D \triangleq 2RT + 1. \quad (4)$$

Given the past N_P observations, the model input is the windowed tensor

$$\mathbf{X}_t \in \mathbb{R}^{N_P \times D}. \quad (5)$$

We predict future channel *increments* over a horizon of N_L steps. Specifically, increments are defined in the complex channel domain as

$$\Delta \mathbf{H}_{t+k}^{(\text{eff})} \triangleq \mathbf{H}_{t+k}^{(\text{eff})} - \mathbf{H}_{t+k-1}^{(\text{eff})}, \quad k = 1, \dots, N_L. \quad (6)$$

Each increment is represented in real-valued vectorized form for learning. Accordingly, the predictor outputs the multi-step increment tensor

$$\mathbf{Y}_t \in \mathbb{R}^{N_L \times C}, \quad C \triangleq 2RT. \quad (7)$$

Increment prediction reduces the dynamic range by removing slowly varying components and stabilizes learning.

III. PROPOSED GRU-ATTENTION-DSLH PREDICTOR

The proposed architecture combines a GRU encoder, Luong-style attention, and bottleneck gated fusion, followed by a DSLH that maps the refined sequence to the N_L -step prediction horizon.

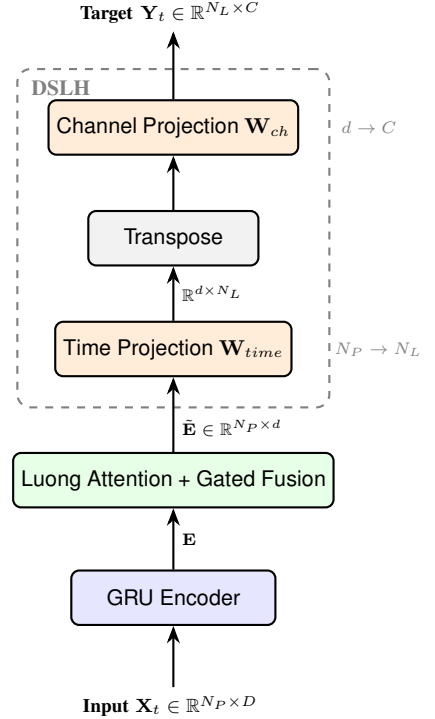


Fig. 1. Overview of the proposed architecture.

A. GRU Encoder

The core of our predictor is a multi-layer GRU network. Compared to LSTMs, GRUs employ fewer gates, reducing parameter count while retaining the ability to model temporal channel coherence. The GRU processes this sequence element-wise, where $\mathbf{x}_\tau = \mathbf{X}_t[\tau, :] \in \mathbb{R}^D$ denotes the input feature vector at the τ -th position within the past window. The GRU maintains a hidden state $\mathbf{h}_\tau \in \mathbb{R}^d$, where d is the GRU hidden dimension.

For each time step $\tau \in \{1, \dots, N_P\}$, the GRU updates are

$$\mathbf{z}_\tau = \sigma(\mathbf{W}_z \mathbf{x}_\tau + \mathbf{U}_z \mathbf{h}_{\tau-1} + \mathbf{b}_z), \quad (8)$$

$$\mathbf{r}_\tau = \sigma(\mathbf{W}_r \mathbf{x}_\tau + \mathbf{U}_r \mathbf{h}_{\tau-1} + \mathbf{b}_r), \quad (9)$$

$$\tilde{\mathbf{h}}_\tau = \tanh(\mathbf{W}_h \mathbf{x}_\tau + \mathbf{U}_h (\mathbf{r}_\tau \odot \mathbf{h}_{\tau-1}) + \mathbf{b}_h), \quad (10)$$

$$\mathbf{h}_\tau = (1 - \mathbf{z}_\tau) \odot \mathbf{h}_{\tau-1} + \mathbf{z}_\tau \odot \tilde{\mathbf{h}}_\tau, \quad (11)$$

where $\mathbf{z}_\tau \in \mathbb{R}^d$ and $\mathbf{r}_\tau \in \mathbb{R}^d$ are the update and reset gates, respectively; $\tilde{\mathbf{h}}_\tau \in \mathbb{R}^d$ is the candidate hidden state; $\sigma(\cdot)$ is the element-wise sigmoid; $\tanh(\cdot)$ is the element-wise hyperbolic tangent; and \odot denotes the Hadamard (element-wise) product. The trainable parameters are $\mathbf{W}_z, \mathbf{W}_r, \mathbf{W}_h \in \mathbb{R}^{d \times D}$, $\mathbf{U}_z, \mathbf{U}_r, \mathbf{U}_h \in \mathbb{R}^{d \times d}$, and biases $\mathbf{b}_z, \mathbf{b}_r, \mathbf{b}_h \in \mathbb{R}^d$.

Stacking the hidden states yields the encoder output sequence

$$\mathbf{E} = [\mathbf{h}_1, \dots, \mathbf{h}_{N_P}]^\top \in \mathbb{R}^{N_P \times d}, \quad (12)$$

B. Scaled Luong Attention with Gated Fusion

To capture long-range dependencies without the quadratic cost of self-attention, we employ a global attention mechanism based on *Luong dot-product attention* [14]. Unlike standard approaches that pool the sequence into a single vector, we

compute an *attention-refined sequence* $\tilde{\mathbf{E}}$ that preserves the temporal structure required by the DSLH.

We use the final hidden state \mathbf{h}_{N_P} as the query vector \mathbf{q} , following the global attention formulation of Luong et al. [14]. Scaled dot-product attention scores are computed as

$$\alpha_\tau = \frac{\mathbf{h}_\tau^\top \mathbf{q}}{\sqrt{d}}, \quad w_\tau = \frac{\exp(\alpha_\tau)}{\sum_{j=1}^{N_P} \exp(\alpha_j)}, \quad (13)$$

where α_τ denotes the unnormalized attention score measuring the relevance of the τ -th encoder hidden state to the query, and the scaling factor \sqrt{d} is adopted for numerical stability, as in Transformer-style attention [15]. The resulting context vector

$$\mathbf{c} = \sum_{j=1}^{N_P} w_j \mathbf{h}_j \quad (14)$$

summarizes the relevant history under the Luong global attention scheme.

A *Bottleneck Gated Fusion* module [16], [17] integrates this context back into the sequence with minimal parameter overhead:

$$\mathbf{u}_\tau = [\mathbf{h}_\tau; \mathbf{c}], \quad (15)$$

$$\mathbf{g}_\tau = \sigma(\mathbf{W}_2 \text{ReLU}(\mathbf{W}_1 \mathbf{u}_\tau)), \quad (16)$$

$$\mathbf{h}'_\tau = \mathbf{g}_\tau \odot \mathbf{h}_\tau + (1 - \mathbf{g}_\tau) \odot \mathbf{c}, \quad (17)$$

where $\mathbf{W}_1 \in \mathbb{R}^{\frac{d}{r} \times 2d}$ and $\mathbf{W}_2 \in \mathbb{R}^{d \times \frac{d}{r}}$ constitute the bottleneck with reduction ratio r . Here, $\text{ReLU}(\cdot)$ is the Rectified Linear Unit; and $\mathbf{g}_\tau \in \mathbb{R}^d$ is the learnable fusion gate that dynamically balances local temporal features and global context. Because (17) produces \mathbf{h}'_τ for every encoder step τ , the model passes a refined sequence $\tilde{\mathbf{E}} \in \mathbb{R}^{N_P \times d}$ to the prediction head rather than a pooled vector. This is structurally compatible with the DSLH, whose time projection mixes encoder positions and whose channel projection maps feature dimensions. Accordingly, the DSLH serves here as a compact sequence-to-sequence output head rather than a generic replacement for any dense predictor.

C. Dimension-wise Separable Linear Head (DSLH)

A conventional dense output head that directly maps the encoder output $\tilde{\mathbf{E}} \in \mathbb{R}^{N_P \times d}$ to the future sequence $\hat{\mathbf{Y}}_t \in \mathbb{R}^{N_L \times C}$ is parameter-heavy, particularly when the prediction horizon N_L and output dimension C are large. We adopt the *Dimension-wise Separable Linear Head* (DSLH) proposed in LinFormer [8], which factorizes the output mapping into decoupled projections along the temporal and channel dimensions.

DSLH consists of two linear mappings:

- *Time projection*: $\mathbf{W}_{\text{time}} \in \mathbb{R}^{N_P \times N_L}$, which linearly mixes the N_P encoder positions to produce N_L future positions.
- *Channel projection*: $\mathbf{W}_{\text{ch}} \in \mathbb{R}^{d \times C}$, which maps the feature dimension d to the output dimension C .

The prediction is computed in two steps. First, a temporal projection is applied:

$$\mathbf{G} \triangleq \mathbf{W}_{\text{time}}^\top \tilde{\mathbf{E}} \in \mathbb{R}^{N_L \times d}, \quad (18)$$

which aggregates information from the past window into N_L future-aligned representations. Second, a channel projection is applied to each future step:

$$\hat{\mathbf{Y}}_t \triangleq \mathbf{G} \mathbf{W}_{\text{ch}} \in \mathbb{R}^{N_L \times C}. \quad (19)$$

Equivalently, the overall mapping can be written as

$$\hat{\mathbf{Y}}_t = \left(\tilde{\mathbf{E}}^\top \mathbf{W}_{\text{time}} \right)^\top \mathbf{W}_{\text{ch}}. \quad (20)$$

Compared to a dense mapping from $\mathbb{R}^{N_P d}$ to $\mathbb{R}^{N_L C}$ with $N_P d N_L C$ parameters, DSLH requires only $N_P N_L + dC$ parameters (excluding biases).

IV. PERFORMANCE EVALUATION

We evaluate the proposed model under 3GPP TR 38.901 channel conditions against GRU, LSTM, and LinFormer baselines. All models use the same hidden dimension, the same DSLH head, and UE speed as an additional input to provide a controlled comparison under a common output interface.

A. Data and Evaluation Protocol

Channels are generated using QuaDRiGa v2.8.1-0 under standardized 3GPP TR 38.901 UMa/UMi LOS and NLOS scenarios [18], [19]. Each run simulates a UE moving along a 150 m linear trajectory at 30 snapshots/m for a 3.5 GHz carrier. QuaDRiGa produces a channel tensor in $\mathbb{C}^{R \times T \times P \times T_s}$, where P denotes the number of multipath components and T_s the number of time snapshots.

All experiments use a 2×2 MIMO setup ($R = T = 2$), yielding $D = 9$ input features per time step and $C = 8$ real-valued output dimensions. The evaluation protocol is based on standardized 3GPP TR 38.901 urban macro (UMa) and urban micro (UMi) environments, with held-out test scenarios covering general mixed-condition evaluation, pedestrian mobility, challenging UMi NLOS propagation, high-speed mobility, and favorable UMa LOS conditions, as summarized in Table I. Sliding windows with $N_P = 128$ and $N_L = 8$ produce approximately 900k training and 200k validation windows from the mixed training set.

TABLE I
TRAINING AND TESTING SCENARIOS USED IN SECTION IV.

ID	Phase	Environment	Speed (km/h)
–	Training	UMa/UMi (LOS/NLOS)	3–60
Scenario I	Testing	UMa LOS + UMi NLOS	10–60
Scenario II	Testing	UMi (LOS/NLOS)	3–5
Scenario III	Testing	UMi NLOS	10–60
Scenario IV	Testing	UMa (LOS/NLOS)	80–120
Scenario V	Testing	UMa LOS	10–60

B. Metrics and Experimental Setup

Prediction accuracy is evaluated using sample-weighted NMSE (dB) as the primary metric, with per-frame MSE tracked at each future step $k = 1, \dots, N_L$. Training minimizes a weighted MSE loss with decaying weights $w_k = k^{-1/2}$. A 200-sample gap between training and validation segments

prevents data leakage, and normalization statistics are derived from training data only. All results are averaged over 10 independent runs; tables report Mean \pm Std.

The key simulation parameters, model configurations, and training hyperparameters used across all experiments are summarized in Table II.

TABLE II
SIMULATION AND HYPERPARAMETER CONFIGURATION

Parameter	Value	Parameter	Value
Past Window (N_P)	128	Hidden Dim (d)	256
Future Horizon (N_L)	8	Network Layers	3
Train/Val Split	80/20%	FFN Multiplier [†]	4 \times
Batch Size	256	Dropout Rate	0.3
Max Epochs	100	Reduction Ratio	4
Learning Rate	3×10^{-4}	Patience	15
Weight Decay	1×10^{-4}	Random Seeds	10

[†] Specific to LinFormer architecture.

C. Comparative Performance Evaluation with Benchmarks

Table III reports efficiency on an NVIDIA RTX A2000 (batch size 256). At $N_P = 128$ with matched dimensions, GRU baseline achieves up to $2.8\times$ higher throughput than LinFormer, while the proposed model attains competitive or better NMSE across several scenarios (Table IV).

TABLE III
MODEL COMPLEXITY, EFFICIENCY, AND THROUGHPUT

Model	Params (M)	Complexity (GFLOPs)	Throughput (samples/s)	Avg NMSE (dB)
LinFormer	1.68	0.40	5,811.07	-13.86 \pm 0.26
LSTM	1.59	0.41	12,738.40	-11.73 \pm 0.03
GRU	1.19	0.31	16,143.51	-12.33 \pm 0.07
Proposed	1.24	0.32	13,162.90	-13.84 \pm 0.15

Table IV shows that the proposed model attains the best mean NMSE in Scenario I, II, and V, indicating that its advantages are most pronounced in general, pedestrian, and LOS-dominant settings. In Scenario V, the proposed model outperforms LinFormer (-18.27 vs. -17.73 dB) while exhibiting lower variance (± 0.25 vs. ± 0.60). In Scenario II, it also achieves the best performance with -16.26 dB compared to LinFormer’s -16.06 dB. By contrast, LinFormer performs best in Scenario III and narrowly in Scenario IV. Notably, Scenario IV lies outside the training speed range (80–120 km/h vs. 3–60 km/h), yet the proposed model remains competitive, trailing by only 0.14 dB (-10.81 vs. -10.95 dB).

Fig. 2 illustrates the prediction error growth over the future horizon, averaged across all test scenarios. While LinFormer achieves the lowest error at the earliest prediction steps (Steps 1–3), the performance gap narrows significantly toward the later steps (Steps 4–8). Throughout the entire horizon, the proposed model remains consistently better than the GRU and LSTM baselines. Interpreted jointly with the throughput results in Table III, the proposed model provides a highly favorable accuracy–latency trade-off, surpassing LinFormer in three out of five scenarios while running $2.3\times$ faster.

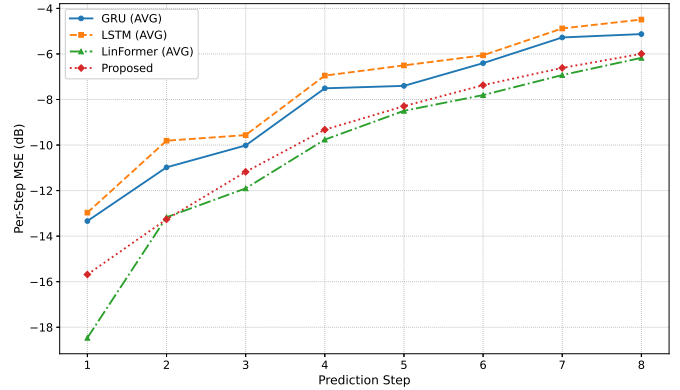


Fig. 2. NMSE over time (average across all test scenarios).

D. Training Cost

Table V compares training efficiency across models. Total training time reflects early stopping and therefore depends on both per-epoch cost and the number of epochs completed. The proposed model requires more training time than GRU (5431 s vs. 3947 s) due to the attention and gated fusion components, but substantially less than LinFormer (8126 s) and at nearly half the GPU memory (567 MB vs. 1093 MB).

TABLE V
TRAINING COST COMPARISON ACROSS MODELS

Model	Train Time (s)	Average Epoch (s)	Mem (MB)
GRU	3947 \pm 1209	54.22	543
LSTM	2664 \pm 302	59.45	520
Proposed	5431 \pm 1338	63.95	567
LinFormer	8126 \pm 711	83.84	1093

All training experiments were conducted on an NVIDIA A40, while inference benchmarks were performed on an NVIDIA RTX A2000.

E. Ablation Study

Table VI supports two conclusions. First, replacing fixed linear per-step fusion with gated fusion improves NMSE from -13.18 dB to -13.84 dB while reducing parameters from 1.32M to 1.24M, indicating that learned data-dependent fusion is more effective than a fixed linear projection of the hidden and context vectors in this architecture. Second, DSLH alone on top of a plain GRU is not sufficient, as GRU (DSLH) underperforms GRU (Dense) (-12.33 dB vs. -13.12 dB). However, once the sequence representation is strengthened by attention and gated fusion, DSLH becomes effective, and the full proposed model outperforms GRU (Dense) while yielding the best accuracy–parameter trade-off.

Table VII shows that appending UE speed consistently improves NMSE across all scenarios, with gains ranging from 0.65 dB (Scenario IV) to 1.72 dB (Scenario III). The largest improvements are observed in NLOS and LOS scenarios (Scenario III and V), indicating that speed provides useful information that enhances the model’s performance.

TABLE IV
PERFORMANCE BENCHMARK (NMSE IN DB) WITH MEAN \pm STD ACROSS TEST SCENARIOS

Model	Scenario I	Scenario II	Scenario III	Scenario IV	Scenario V
LSTM	-12.87 \pm 0.14	-13.34 \pm 0.22	-7.86 \pm 0.09	-8.80 \pm 0.36	-15.77 \pm 0.23
GRU	-13.43 \pm 0.15	-14.14 \pm 0.15	-8.52 \pm 0.05	-9.21 \pm 0.21	-16.36 \pm 0.19
LinFormer	-14.48 \pm 0.22	-16.06 \pm 0.33	-10.07 \pm 0.19	-10.95 \pm 0.19	-17.73 \pm 0.60
Proposed	-14.60 \pm 0.20	-16.26 \pm 0.23	-9.26 \pm 0.16	-10.81 \pm 0.11	-18.27 \pm 0.25

TABLE VI
ABLATION STUDY OF ARCHITECTURAL COMPONENTS

Variant	Params (M)	Avg. NMSE (dB)
GRU (Dense) ^a	3.28	-13.12 \pm 0.15
GRU (DSLH)	1.19	-12.33 \pm 0.07
GRU+Attn (Dense) ^a	3.42	-13.25 \pm 0.21
GRU+Attn+Gated Fusion (Dense) ^a	3.33	-13.31 \pm 0.13
GRU+Attn (DSLH) ^b	1.32	-13.18 \pm 0.27
Proposed^c	1.24	-13.84 \pm 0.15

^a Dense denotes a direct mapping from the full refined sequence to the $N_L \times C$ output.

^b GRU+Attn (DSLH) uses fixed linear per-step fusion $W[h_\tau; c]$.

^c Proposed uses gated fusion.

TABLE VII
IMPACT OF UE SPEED INPUT ON NMSE (DB) ACROSS TEST SCENARIOS

Scenario	Proposed	No Speed
Scenario I	-14.60 \pm 0.20	-13.78 \pm 0.31
Scenario II	-16.26 \pm 0.23	-14.91 \pm 0.30
Scenario III	-9.26 \pm 0.16	-7.54 \pm 0.20
Scenario IV	-10.81 \pm 0.11	-10.16 \pm 0.23
Scenario V	-18.27 \pm 0.25	-16.88 \pm 0.35

V. CONCLUSION

This letter presented a resource-efficient CSI predictor based on a GRU backbone, gated attention fusion, and a Dimension-wise Separable Linear Head (DSLH). Under 3GPP TR 38.901 channel simulations, the proposed model achieved an average NMSE of -13.84 dB while reducing parameters by 26% and increasing inference throughput by approximately $2.3\times$ relative to a dimension-matched LinFormer baseline. The results indicate that the proposed architecture offers a competitive accuracy–efficiency trade-off for short-horizon CSI prediction, with particularly favorable performance in several LOS and mixed-condition scenarios. These findings suggest that, under the evaluated short-horizon 3GPP setting, lightweight recurrent models with structured output heads remain competitive alternatives to the considered LinFormer baseline. Future work will extend the study to wideband OFDM settings.

REFERENCES

- [1] B. V. Boas, W. Zirwas, and M. Haardt, "Machine learning based channel prediction for nr type ii csi reporting," in *ICC 2023 - IEEE International Conference on Communications*, 2023, pp. 4967–4972.
- [2] H. Lee, J. Jeong, and M. Frenne, "Predictive channel state information (csi) framework: Evolutional csi neural network (evocsinet)," in *2024 IEEE International Conference on Machine Learning for Communication and Networking (ICMLCN)*, 2024, pp. 311–316.
- [3] M. K. Shehzad, L. Rose, M. F. Azam, and M. Assaad, "Real-time massive mimo channel prediction: A combination of deep learning and neuralprophet," in *GLOBECOM 2022 - IEEE Global Communications Conference*, 2022, pp. 1423–1428.
- [4] S. Kadambar, A. K. Reddy Chavva, C. Lim, A. Goyal, D. Singh, A. Kumar, and S. R. Bal, "Smart-csi: Deep learning based low complexity csi prediction for beyond-5g systems," in *2023 IEEE 98th Vehicular Technology Conference (VTC2023-Fall)*, 2023, pp. 1–5.
- [5] N. Mehrnia, P. Valiahdi, S. Coleri, and J. Gross, "Channel prediction using deep recurrent neural network with evt-based adaptive quantile loss function," *IEEE Communications Letters*, vol. 29, no. 7, pp. 1699–1703, 2025.
- [6] H. Jiang, M. Cui, D. W. K. Ng, and L. Dai, "Accurate channel prediction based on transformer: Making mobility negligible," *IEEE Journal on Selected Areas in Communications*, vol. 40, no. 9, pp. 2717–2732, 2022.
- [7] Z. Xiao, Y. Huang, Y. Xu, T. Jiao, and D. He, "Ode-former for mobile channel prediction: A novel learning structure leveraging the physics continuity," *IEEE Wireless Communications Letters*, vol. 14, no. 7, pp. 2184–2188, 2025.
- [8] Y. Jin, Y. Wu, Y. Gao, S. Zhang, S. Xu, and C.-X. Wang, "Linformer: A linear-based lightweight transformer architecture for time-aware mimo channel prediction," *IEEE Transactions on Wireless Communications*, vol. 24, no. 9, pp. 7177–7190, 2025.
- [9] O. Stenhammar, G. Fodor, and C. Fischione, "A comparison of neural networks for wireless channel prediction," *IEEE Wireless Communications*, vol. 31, no. 3, pp. 235–241, 2024.
- [10] S. Hakimi, G. Berardinelli, and R. Adeogun, "Attention-aided channel prediction for efficient resource management in industrial iot subnetworks," *IEEE Internet of Things Journal*, vol. 12, no. 22, pp. 48 304–48 317, 2025.
- [11] X. Hu, Y. Huo, X. Dong, F.-Y. Wu, and A. Huang, "Channel prediction using adaptive bidirectional gru for underwater mimo communications," *IEEE Internet of Things Journal*, vol. 11, no. 2, pp. 3250–3263, 2024.
- [12] L. Cai, G. Xu, and D. Niyato, "Att-gru: An attention-enhanced gated recurrent unit for channel prediction in deep space communications," *IEEE Transactions on Vehicular Technology*, pp. 1–6, 2025.
- [13] R. Kumar and M. Rathinam, "An eran-based dynamic graph neural network for csi prediction in massive mimo systems," *IEEE Wireless Communications Letters*, vol. 14, no. 11, pp. 3560–3564, 2025.
- [14] M.-T. Luong, H. Pham, and C. D. Manning, "Effective approaches to attention-based neural machine translation," in *Proceedings of the Conference on Empirical Methods in Natural Language Processing (EMNLP)*, 2015, pp. 1412–1421, available: <https://arxiv.org/abs/1508.04025>.
- [15] A. Vaswani, N. Shazeer, N. Parmar, J. Uszkoreit, L. Jones, A. N. Gomez, L. Kaiser, and I. Polosukhin, "Attention is all you need," 2023. [Online]. Available: <https://arxiv.org/abs/1706.03762>
- [16] J. Hu, L. Shen, S. Albanie, G. Sun, and E. Wu, "Squeeze-and-excitation networks," 2019. [Online]. Available: <https://arxiv.org/abs/1709.01507>
- [17] Y. N. Dauphin, A. Fan, M. Auli, and D. Grangier, "Language modeling with gated convolutional networks," 2017. [Online]. Available: <https://arxiv.org/abs/1612.08083>
- [18] S. Jaeckel, L. Raschkowski, K. Börner, L. Thiele, F. Burkhardt, and E. Eberlein, "QuaDRiGa – Quasi Deterministic Radio Channel Generator, User Manual and Documentation," Fraunhofer Heinrich Hertz Institute, Technical Report, 2019. [Online]. Available: <https://quadriga-channel-model.de/>
- [19] 3rd Generation Partnership Project (3GPP), "Study on channel model for frequencies from 0.5 to 100 GHz," 3rd Generation Partnership Project (3GPP), Technical Report (TR) 38.901, 2020. [Online]. Available: <https://www.3gpp.org/dynareport/38901.html>